Bioorganic & Medicinal Chemistry Letters 19 (2009) 1195–1198

Contents lists available at ScienceDirect

Bioorganic & Medicinal Chemistry Letters

journal homepage: www.elsevier.com/locate/bmcl

3,4-Disubstituted isothiazoles: Novel potent inhibitors of VEGF receptors 1 and 2

Alexander S. Kiselyov [a,*], Marina Semenova [b], Victor V. Semenov [c]

[a] deCODE, 2501 Davey Road, Woodridge, IL 60616, USA
[b] Institute of Developmental Biology, RAS, 26 Vavilov Str., 119334 Moscow, Russia
[c] Zelinsky Institute of Organic Chemistry, RAS, 47 Leninsky Prospect, 117913 Moscow, Russia

ARTICLE INFO

Article history:
Received 10 December 2008
Accepted 17 December 2008
Available online 24 December 2008

Keywords:
Angiogenesis
ATP-competitive kinase inhibitors
Vascular endothelial growth factor receptor 2
VEGFR-2
Isothiazoles

ABSTRACT

Novel derivatives of isothiazoles are described as potent ATP-competitive inhibitors of vascular endothelial growth factor receptors I and II (VEGFR-1/2). A number of compounds exhibited VEGFR-2 inhibitory activity comparable to that of Vatalanib™ in both HTRF enzymatic and cellular assays. Several derivatives featuring bulky meta-substituents in the amide portion of the molecule displayed 4- to 8-fold specificity for VEGFR-2 versus VEGFR-1. Active molecules also showed high intrinsic permeability (>30 × 10^{-5} cm/min) across Caco-2 cell monolayer.

Cancer cells easily acquire resistance towards conventional cytotoxic agents commonly used for chemotherapy.[1] It is believed that this issue could be addressed by anti-angiogenesis therapy targeting tumor vascular endothelial cells.[2] Angiogenesis, or formation of new blood vessels, is a process critical to both development and systems maintenance in vertebrates.[3] Vascular endothelial growth factors (VEGFs) and their respective family of receptor tyrosine kinases (VEGFRs) are key proteins regulating vascular development during angiogenesis.[4–10] These include receptor tyrosine kinases, VEGFR-1 (Flt-1) and VEGFR-2 (Kinase Insert Domain Receptor (KDR) or flk1).[10–13] In early embryogenesis, VEGFR-1 functions as a negative regulator, most likely through its strong VEGF-A trapping activity. In adults, VEGFR-1-specific ligands are reported to induce mild angiogenesis. VEGFR-2 is the major positive signal transducer for endothelial cell proliferation and differentiation at all mammalian stages of development.[11] There has been considerable in vivo evidence, including clinical observations, that the abnormal angiogenesis is implicated in a number of malignancies, which include rheumatoid arthritis, inflammation, cancer, degenerative eye conditions and others. Potent, specific and non-toxic inhibitors of angiogenesis were reported to be powerful clinical tools in oncology and ophthalmology.[12,13]

Several groups in the industry have developed methods for sequestering VEGF which leads to a signal blockade via VEGF receptors and, subsequently to an inhibition of a malignant angiogenesis. Perhaps, the most successful marketed agent reportedly working via this mechanism is Avastin™.[14] A number of small-molecule inhibitors are known to affect VEGF/VEGFR signaling. These include PTK787 (Vatalanib™ **A**),[15] its analog BAY579352 (**B**),[16] and the isosteric anthranyl amide derivatives **C**[17] and AMG-706 (**D**).[18] Intramolecular hydrogen bonding in **C** and **D** was suggested[17,19] to be responsible for the optimal spatial orientation of the pharmacophore pieces, similar to that of the parent PTK787 (Fig. 1).

The essential pharmacophore elements for the VEGFR-2 activity of phthalazine-based molecules and their analogs (**A–D**) include[20] (i) [6,6]fused (or related) aromatic system; (ii) *para*- or 3,4-disubstituted aniline function in position 1 of the phthalazine core; (iii) hydrogen bond acceptor (Lewis' base: lone pair(s) of a nitrogen- or oxygen atom(s)) attached to position 4 via an appropriate linker (aryl or fused aryl group). In this communication, we expand upon our initial findings[19,20] and disclose potent inhibitors of VEGFR-2 kinase based on thiazoles. We reasoned that this template could provide for the both proper pharmacophore arrangement and favorable ex vivo PK profile.

Results and discussion: A series of isothiazoles **3–32** (Scheme 1 and Table 1) were synthesized as described in Scheme 1. Reaction sequence involving formation of a respective amide from the cyanoacetic ester and preparation of the respective oxime was followed by the cyclization of the resulting cyanamide with EtO_2CH_2SH to furnish isothiazoles **1** featuring desired arrangements of the tether groups. Carbetoxy moiety in **1** was removed to afford **2**, the key precursor to targeted heterocycles. Reductive amination of **2** with a series of aldehydes furnished isothiazoles **3–32** in a 28–52% overall yield.[21]

* Corresponding author. Tel.: +1 630 783 4900.
E-mail address: akiselyov@decode.com (A.S. Kiselyov).

0960-894X/$ - see front matter © 2008 Elsevier Ltd. All rights reserved.
doi:10.1016/j.bmcl.2008.12.078

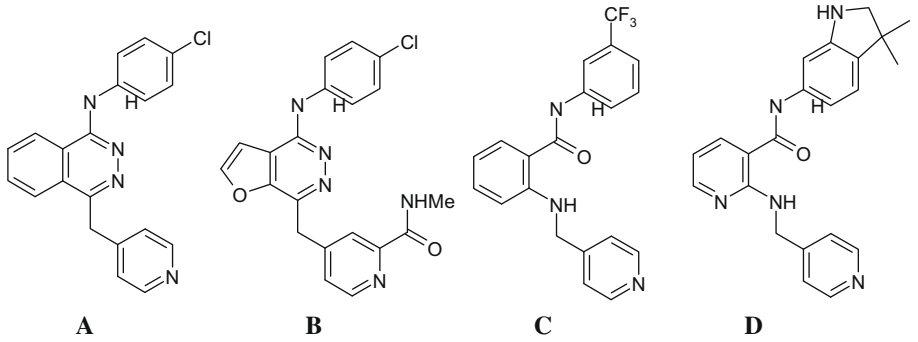

Figure 1. Selected Inhibitors of VEGFR-2.

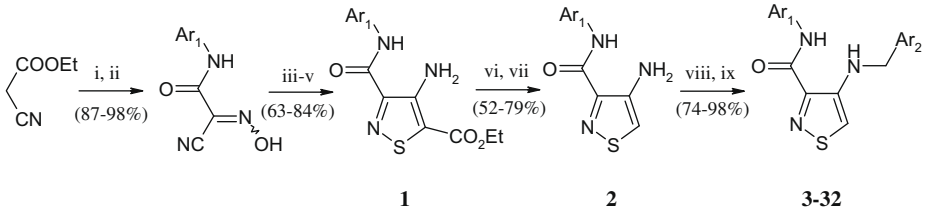

Scheme 1. Synthesis and activity of thiazoles **3**–**32** against VEGFR-2 and VEGFR-1 kinases in vitro and in cell-based assays. Reagents and conditions: (i) Ar^1–NH_2, Im, EtOH, 200 °C; (ii) EtONO, EtONa, EtOH; (iii) TsCl, Py, benzene, −78 °C; (iv) EtO_2CCH_2SH, Py, EtOH, 25 °C; (v) Et_3N, 25 °C; (vi) NaOH, EtOH, 22 h, 25 °C; (vii) NaOH, H_2O, 0.5 h, 25 °C; (viii) Ar^2–CHO, AcOH, MeOH; (ix) $NaBH_4$, MeOH.

Table 1
Activity of thiazoles **3**–**32** against VEGFR-2 and VEGFR-1 kinases in vitro and in cell-based assays

Compound	Ar^1	Ar^2	VEGFR-2, enzymatic, IC_{50}, μM[a]	VEGFR-1, enzymatic, IC_{50}, μM[a]	VEGFR-2, cell-based ELISA, IC_{50}, μM[a,b,c]
A, **PTK787** Vatalanib™**C**			0.054 ± 0.006 (0.042 ± 0.003)[b] 0.032 ± 0.005 (0.023 ± 0.006)[b]	0.14 ± 0.02 (0.11 ± 0.03)[b] 0.17 ± 0.05 (0.130 ± 0.081)[b]	0.021 ± 0.03 (0.016 ± 0.001)[b] 0.09 ± 0.01 (0.0012 ± 0.0002)[b]
3	**3-$F_3C(C_6H_4)$**	**4-Pyridine**	**0.041 ± 0.006**	**0.17 ± 0.02**	**0.054 ± 0.01**[d]
4	3-$F_3C(C_6H_4)$	3-Pyridine	4.23 ± 0.51	>10	>10
5	3-$F_3C(C_6H_4)$	2-Pyridine	>10	>10	>10
6	4-$F_3C(C_6H_4)$	4-Pyridine	0.21 ± 0.04	0.25 ± 0.08	1.53 ± 0.24
7	4-$F_3C(C_6H_4)$	3-Pyridine	>10	>10	>10
8	4-$F_3C(C_6H_4)$	2-Pyridine	>10	>10	>10
9	**3-$F_3CO(C_6H_4)$**	**4-Pyridine**	**0.033 ± 0.005**	**0.26 ± 0.05**	**0.041 ± 0.02**
10	4-$F_3CO(C_6H_4)$	4-Pyridine	0.46 ± 0.07	1.23 ± 0.11	0.77 ± 0.12
11	**3-*t*Bu-(C_6H_4)**	**4-Pyridine**	**0.035 ± 0.007**	**0.31 ± 0.03**	**0.082 ± 0.06**
12	4-*t*Bu-(C_6H_4)	4-Pyridine	0.36 ± 0.07	0.61 ± 0.09	1.15 ± 0.11
13	4-Cl-(C_6H_4)	4-Pyridine	0.14 ± 0.05	0.25 ± 0.06	0.42 ± 0.11
14	**3-Br-(C_6H_4)**	**4-Pyridine**	**0.027 ± 0.004**	**0.055 ± 0.005**	**0.21 ± 0.07**
15	4-Br-(C_6H_4)	4-Pyridine	0.23 ± 0.08	0.26 ± 0.05	1.04 ± 0.16
16	2-Br-(C_6H_4)	4-Pyridine	>10	>10	>10
17	2-(Quinolinyl)	4-Pyridine	0.44 ± 0.08	0.38 ± 0.07	0.77 ± 0.12
18	5-(Indazolyl)	4-Pyridine	0.82 ± 0.13	1.09 ± 0.22	>10
19	3-F_3C,4-Cl(C_6H_4)	4-Pyridine	0.23 ± 0.06	0.98 ± 0.16	0.53 ± 0.09
20	3-Cl,4-$F_3C(C_6H_4)$	4-Pyridine	0.89 ± 0.15	1.80 ± 0.24	2.05 ± 0.33
21	3,4-di-Cl(C_6H_4)	4-Pyridine	0.67 ± 0.10	0.75 ± 0.12	1.11 ± 0.24
22	**4-Me-3-$F_3C(C_6H_3)$**	**4-Pyridine**	**0.043 ± 0.09**	**0.19 ± 0.05**	**0.056 ± 0.02**
23	3-Me-4–$F_3C(C_6H_3)$	4-Pyridine	0.49 ± 0.12	0.67 ± 0.11	0.71 ± 0.18
24	2-F-4-Me(C_6H_3)	4-Pyridine	1.98 ± 0.28	2.51 ± 0.22	1.89 ± 0.33
25	Piperonyl-	4-Pyridine	0.65 ± 0.19	0.70 ± 0.11	0.79 ± 0.21
26	3-$F_3C(C_6H_4)$	3,4-di-F-(C_6H_3)	>10	>10	>10
27	3-$F_3C(C_6H_4)$	5-Piperonyl	>10	>10	>10
28	3-Br-(C_6H_4)	5-Piperonyl	>10	>10	>10
29	**3-Br-(C_6H_4)**	**4-Quinolyl**	**0.15 ± 0.06**	**0.33 ± 0.09**	**0.27 ± 0.07**
30	**3-$F_3C(C_6H_4)$**	**4-Quinolyl**	**0.11 ± 0.02**	**0.58 ± 0.15**	**0.39 ± 0.14**
31	3-Br-(C_6H_4)	4-Isoxazolo	>10	>10	>10
32	3-Br-(C_6H_4)	2-Quinolyl	>10	>10	>10

[a] IC_{50} values were determined from the logarithmic concentration-inhibition point (ten points).[22] The important values are given as the mean of at least two duplicate experiments.
[b] *Lit*. IC_{50} values, as measured at 8 μM ATP.
[c] *Lit*. data correspond to the inhibition of VEGF-induced phosphorylation of VEGFR-2 in CHO cells.
[d] Molecules with best enzymatic and cellular potencies against VEGFR-2 are bolded.[22,23]

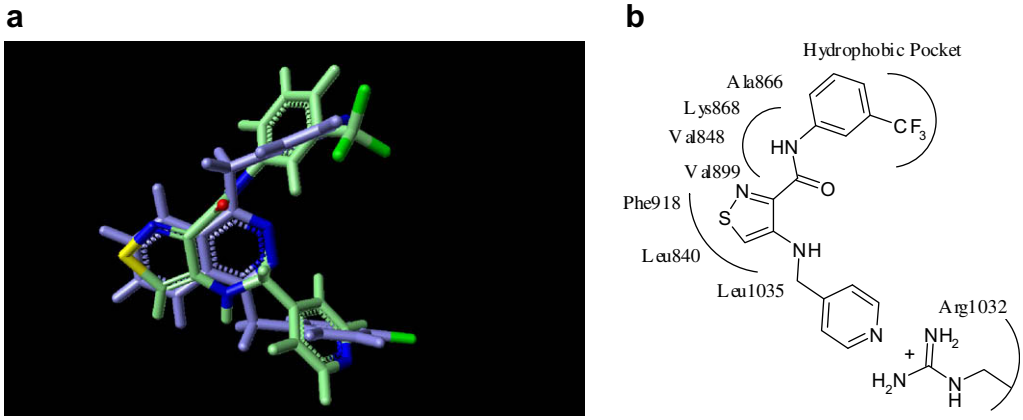

Figure 2. Structural overlap between (a) **3** (green) and Vatalanib™ (blue); (b) pharmacophore hypothesis for the mode of binding of isothiazole **3** within the ATP-binding pocket of VEGFR-2. Central aromatic ring is surrounded by *Leu*840, *Val*848, *Val*899, *Phe*918 and *Leu*1035. The amide is in close proximity with the *Ala*866 and *Lys*868, and pyridine nitrogen is near *Arg*1032.

Thirty compounds (**3–32**, Table 1) were first tested in vitro against isolated VEGFR-2.[22] Specifically, we measured their ability to inhibit phosphorylation of a biotinylated-polypeptide substrate (p-GAT, CIS Bio International) in a homogenous time-resolved fluorescence (HTRF) assay at an ATP-concentration of 2 μM. The results were reported as a 50% inhibition concentration value (IC_{50}). Literature VEGFR-2 inhibitors including Vatalanib™ and **C** (Fig. 1) were used as internal standards for quality control.

As can be seen from Table 1, majority of isothiazoles exhibited good inhibitory activity against VEGFR-2.[22] By varying substituents at both Ar^1 and Ar^2 moieties it was possible to modulate compounds' potency against the enzyme. In studying SAR of the amide pharmacophore (Ar^1), we found that compounds featuring *meta*-substituted Ar^1 exemplified by *m*-CF_3– (**3**), *m*-OCF_3 (**9**), *m*-*t*-Bu (**11**) and *m*-Br (**14**) displayed better potency with the IC_{50} values of 27–41 nM in the VEGFR-2 enzymatic assay. *Para*-substitution in this portion of the molecule was somewhat tolerated, however the respective analogs were >5-fold less active against the enzyme (Table 1, compare **3** and **6, 9** and **10, 11** and **12**). Comparison of *ortho*-, *meta*- and *para*-functionalized aryl derivatives with the same Ar^1 moiety in VEGFR-2 enzymatic assay (Table 1, compounds **14–16**) also suggested superior potency of the *meta*-derivative **14**. Notably, compound **16** was completely inactive in both in vitro and in the cellular assay.

In order to further explore steric requirements for the Ar^1 substituent, we prepared a series of amides with heterocyclic (Table 1, **17 and 18**) and disubstituted functionalities (**19**–**25**). Specifically, neither 2-(quinolinyl) (**17**) nor 5-(indazolyl) (**18**) Ar^1 improved overall activity of the resulting molecule against the kinase. Isothiazoles featuring 3,4-disubstituted aryl groups consistently displayed reduced potency compared with the respective monosubstituted *meta*-derivatives. However following the trend described above, molecules featuring larger hydrophobic *meta*-substituents were somewhat more active when compared to the respective *para*-analogs (Table 1, compare pairs **19** and **20, 22** and **23**) These facts suggest presence of a relatively tight hydrophobic pocket in the binding site of VEGFR-2.

Table 3
Compounds **3**, **11** and **14** are ATP-competitive inhibitors of VEGFR-2

Compound	K_i at IC_{50} (μM)	K_i at IC_{90} (μM)
3	0.16	0.13
11	0.13	0.12
15	0.09	0.07

In the next series of experiments, we optimized the aniline substituent Ar^2 (Table 1, entries **3–8, 26–32**). Similar to the earlier findings,[19,20] 4-pyridyl group was featured in the most active molecules. 4-Quinolinyl derivatives (**29 and 30**) displayed moderate activity against VEGFR-2, even with the optimized Ar^1 functionality. The combined SAR data indicate that (i) substitution pattern on the Ar^1 group of the amide (compare **3** and **6, 9** and **10, 11** and **12**) and (ii) nature of the aniline substituent Ar^2 (compare **3, 4** and **5, 26–28** and **29**) are critical to the VEGFR-2 inhibitory activity of these new series. It is likely that proper alignment of the lower portion of the molecule, namely nitrogen atoms (Lewis' base, hydrogen bond acceptors) of 4-pyridyl or 4-quinolyl groups (Table 1, for example, **3** and **30**) with the *Arg*1302 moiety in the ATP-binding pocket of VEGFR-2 is required for the activity. We further speculated that the amide function is accommodated in a well-defined binding pocket lined up with *Ala*866 and *Lys* 868. This allows for a better fit of a *meta*-substituted aryl moiety in the hydrophobic pocket of the ATP-binding site of the kinase.[19,20] MMFF94 Force Field minimization studies suggested good overlap between our molecule (**3**) and the development candidate Vatalanib™ (Fig. 2a). Observed structure–activity relationship of the novel isothiazoles **3–32** are in line with the proposed pharmacophore hypothesis (Fig. 2b).

Compounds **3–32** were also tested in HTRF format against VEGFR-1.[22] The results in Table 1 indicate that all VEGFR-2 active isothiazole derivatives (for example, **3, 9, 11, 14, 22, 29, 30**) consistently display good activity against VEGFR-1 with the IC_{50} values in the 31–580 nM range for the most potent compounds. In general, molecules featuring *para*-substituents in the Ar^1 display

Table 2
Passive diffusion potential across Caco-2 cell monolayer for selected compounds

Compound	Intrinsic permeability, P_m value × 10^{-5} cm/min	Absorption potential	Compound	Intrinsic permeability, P_m value × 10^{-5} cm/min	Absorption potential
C	38.6 (lit. 45.2)[18]	High	**14**	32.9	High
3	41.9	Med	**22**	35.4	High
9	47.6	High	**29**	21.5	Med
11	33.5	High	**30**	16.3	Med

VEGFR-2 activity similar to that for the VEGFR-1 (Table 1, for example, **6**, **12**, **13**, **17**). This outcome could be of benefit in the clinical setting as both receptors are reported to mediate VEGF signaling in the angiogenesis.[1–5,20] In our hands, bulky substituents in the *meta*-position of Ar^1 favored VEGFR-2 suggesting potential for the development of an inhibitor selective against VEGFR-1 (Table 1, for example, **3**, **9**, **11**, **22**). Further screening of **3–32** against a number of other receptor (IGF1R, InR, FGFR1, Flt3, EGFR, ErbB2, c-Met, Ron) and cytosolic (PKA, GSK3β, bcr-Abl, bcr-AblT315, Cdk1/2, Src, Auroras A and B, Plk1) kinases in HTRF format indicated no significant cross reactivity (PI < 30%, triplicate measurements) at a concentration of 10 μM.

Active in vitro inhibitors of VEGFR-2 were further characterized in a cell-based phosphorylation ELISA assay (Table 1).[23] In general, good in vitro- to cell-based activity correlation has been found for these compounds. In our hands, the best compounds displayed 41–390 nM activity in inhibiting cell-based phosphorylation of VEGFR-2. Passive diffusion potential for compounds**3, 9, 11, 14, 22, 29, 30** across Caco-2 cell monolayer was predictive of cell permeability. In general, good correlation between cell-based activity and P_m values was observed for all active compounds (Table 2). This fact indicates that a number of derivatives, including **3, 9, 11** could be further developed for in vivo studies.

Further, competition assays were conducted for the selected molecules with varying concentration (0–100 μM) of ATP. Specifically, five different concentrations of ^{32}P ATP were incubated with VEGFR-2 along with varying concentrations (absence, IC_{50}, IC_{90}) of the inhibitors **3, 11** and **14** for 45 min at RT. A double reciprocal graph of the degree of phosphorylation (1/cpm) against ATP-concentration (1/[ATP]) was plotted. The data were analyzed by a non-linear least-squares program to determine kinetic parameters using GraphPad software. Determined K_i values for the three selected compounds are listed in Table 3.

In summary, we have described a series of isothiazoles as potent inhibitors of both VEGFR-2 and VEGFR-1 receptors. Enzymatic and cellular activities of representative molecules are comparable to the clinical candidates Vatalanib™ and AMG-706. This outcome could be of benefit in the clinical setting as both receptors are reported to mediate VEGF signaling in the angiogenesis.

References and notes

1. Bailar, J. C., III; Gornick, H. L. *N. Engl. J. Med.* **1997**, *336*, 1569.
2. Boehm, T.; Folkman, J.; Browder, T. *Nature* **1997**, *390*, 404.
3. Risau, W. *Nature* **1997**, *386*, 671.
4. Klagsbrun, M.; Moses, M. A. *Chem. Biol.* **1999**, *6*, R217.
5. Hanahan, D.; Folkman, J. *Cell* **1996**, *86*, 353.
6. Olsson, A.-K.; Dimberg, A.; Kreuger, J.; Claesson-Welsh, L. *Nat. Rev. Mol. Cell Biol.* **2006**, *5*, 359.
7. Zachary, I. *Biochem. Soc. Trans.* **2003**, *31*, 1171.
8. Perona, R. *Clin. Transl. Oncol.* **2006**, *8*, 77.
9. Jin, T.; Nakatani, H.; Taguchi, T. *World J. Gastroenterol.* **2006**, *12*, 703.
10. Itakura, J.; Ishiwata, T.; Shen, B. *Int. J. Cancer* **2000**, *85*, 27.
11. Saaristo, A.; Karpanen, T.; Alitalo, K. *Oncogene* **2000**, *19*, 6122.
12. Ferrara, N.; Hillan, K. J.; Gerber, H. P.; Novotny, W. *Nat. Rev. Drug Discov.* **2004**, *3*, 391.
13. The anti-angiogenic aptamer Macugen™ (Pegaptanib sodium, Eyetech Pharmaceuticals, New York, NY and Pfizer) has been approved to treat neovascular age-related macular degeneration; see: Fine, S. L.; Martin, D. F.; Kirkpatrick, P. *Nat. Rev. Drug Discov.* **2005**, *4*, 187.
14. The anti-angiogenic antibody Avastin™ (Bevacizumab, Genentech, San Francisco, CA) has been approved for the treatment of colorectal cancer, see: Culy, C. *Drugs Today* **2005**, *41*, 23.
15. Bold, G.; Altmann, K.-H.; Jorg, F.; Lang, M.; Manley, P. W.; Traxler, P.; Wietfeld, B.; Bruggen, J.; Buchdunger, E.; Cozens, R.; Ferrari, S.; Pascal, F.; Hofmann, F.; Martiny-Baron, G.; Mestan, J.; Rosel, J.; Sills, M.; Stover, D.; Acemoglu, F.; Boss, E.; Emmenegger, R.; Lasser, L.; Masso, E.; Roth, R.; Schlachter, C.; Vetterli, W.; Wyss, D.; Wood, J. M. *J. Med. Chem.* **2000**, *43*, 2310.
16. (a) Manley, P. W.; Furet, P.; Bold, G.; Brüggen, J.; Mestan, J.; Meyer, T.; Schnell, C.; Wood, J. *J. Med. Chem.* **2002**, *45*, 5697; (b) Manley, P. W.; Bold, G.; Fendrich, G.; Furet, P.; Mestan, J.; Meyer, T.; Meyhack, B.; Strauss, A.; Wood, J. *Cell. Mol. Biol. Lett.* **2003**, *8*, 532; (c) Altmann, K.-H.; Bold, G.; Furet, P.; Manley, P. W.; Wood, J. M.; Ferrari, S.; Hofmann, F.; Mestan, J.; Huth, A.; Krüger, M.; Seidelmann, D.; Menrad, A.; Haberey, M.; Thierauch, K. -H. US Patent 6,878,720 B2, 2005.
17. Chang, Y. S.; Cortes, C.; Polony, B. Proc. *Am. Assoc. Cancer Res. (AACR)* **2005**, *46*, Abstr 2030.
18. Kaufman, S.; Starnes, C.; Coxon, A. *Proc. Am. Assoc. Cancer Res. (AACR)* **2006**, *47*, Abstr 3792.
19. Kiselyov, A. S.; Piatnitski, L. E.; Samet, A. V.; Kisly, V. P.; Semenov, V. V. *Bioorg. Med. Chem. Lett.* **2007**, *17*, 1369. and references cited therein.
20. Kiselyov, A. S.; Balakin, K.; Tkachenko, S. E. *Exp. Opin. Invest. Drugs* **2007**, *16*, 83.
21. Analytical data for selected compounds—**3**: *4-(Pyridin-4-ylmethylamino)-N-(3-(trifluoromethyl)phenyl)isothiazole-3-carboxamide*; mp 217–219 °C, ^1H NMR (400 MHz, DMSO-d_6) δ, ppm: 4.46 (d, J = 7.2 Hz, 2H), 6.38 (br s, exch. D_2O, 1H, NH), 7.26 (d, J = 8.4 Hz, 1H), 7.35 (d, J = 7.4 Hz, 1H), 7.45 (d, J = 7.6 Hz, 2H), 7.58 (m, 1H), 8.04 (s, 1H), 8.52 (d, J = 5.6 Hz, 2H), 8.79 (s, 1H), 10.38 (br s, exch. D_2O, 1H, NH); ^{13}C NMR (100 MHz, DMSO-d_6) δ, ppm: 45.7, 104.9, 117.7, 120.3, 123.0, 124.1, 124.3, 129.4, 130.9, 135.6, 147.5, 148.1, 150.2, 157.4, 163.7; ESI MS (M+1): 379, (M−1): 377; HRMS, exact mass calcd. for $C_{17}H_{13}F_3N_4OS$: 378.0762, found: 378.0758. Elemental analysis: calcd for $C_{17}H_{13}F_3N_4OS$: C, 53.96; H, 3.46; N, 14.81; found: C, 53.73; H, 3.62, N, 14.58.**11**: *N-(3-tert-butylphenyl)-4-(pyridin-4-ylmethylamino)isothiazole-3-carboxamide*; mp 223–235 °C; ^1H NMR (400 MHz, DMSO-d_6) δ, ppm: 1.25 (s, 9H, *t*Bu), 4.36 (d, J = 7.2 Hz, 2H), 6.48 (br s, exch. D_2O, 1H, NH), 7.07 (d, J = 7.6 Hz, 1H), 7.16–7.18 (m, 2H), 7.42 (d, J = 7.6 Hz, 2H), 7.69 (s, 1H), 8.55 (d, J = 5.6 Hz, 2H), 8.73 (s, 1H), 10.33 (br s, exch. D_2O, 1H, NH); ^{13}C NMR (100 MHz, DMSO-d_6) δ, ppm: 31.2, 40.9, 45.5, 116.9, 118.6, 120.3, 123.2, 124.7, 128.3, 135.7, 147.5, 148.0, 149.6, 149.9, 157.2, 162.1; ESI MS (M+1): 367, (M−1): 365; HRMS, exact mass calcd for $C_{20}H_{22}N_4OS$: 366.1514, found: 366.1512. Elemental analysis: calcd for $C_{20}H_{22}N_4OS$: C, 65.55; H, 6.05; N, 15.29; found: C, 65.41; H, 5.87, N, 15.13. **30**: *4-(quinolin-4-ylmethylamino)-N-(3-(trifluoromethyl)phenyl)isothiazole-3-carboxamide*; mp 250–252 °C; ^1H NMR (400 MHz, DMSO-d_6) δ, ppm: 4.29 (d, J = 7.2 Hz, 2H), 6.51 (br s, exch. D_2O, 1H, NH), 7.01 (dd, J_1 = 8.0 Hz, J_2 = 4.8 Hz, 1H), 7.39 (d, J = 8.4 Hz, 1H), 7.45 (d, J = 7.6 Hz, 1H), 7.59–7.62 (m, 2H), 7.74 (m, 1H), 8.02 (d, J = 6.8 Hz, 1H), 8.13 (s, 1H), 8.19 (d, J = 7.2 Hz, 1H), 8.59 (d, J = 4.8 Hz, 1H), 8.75 (s, 1H), 10.33 (br s, exch. D_2O, 1H, NH); ^{13}C NMR (100 MHz, DMSO-d_6) δ, ppm: 43.5, 117.2, 120.6, 121.8, 123.5, 124.2, 124.6, 124.7, 126.7, 127.4, 129.0, 129.2, 129.5, 130.9, 136.5, 142.0, 146.5, 147.3, 150.3, 156.8, 163.1; ESI MS (M+1): 429, (M−1): 427; HRMS, exact mass calcd for $C_{21}H_{15}F_3N_4OS$: 428.0919, found: 428.0916. Elemental analysis: calcd for $C_{21}H_{15}F_3N_4OS$: C, 58.87; H, 3.53; N, 13.08; found: C, 58.69; H, 3.68, N, 12.91.
22. *VEGFR tyrosine kinase inhibition* is determined by measuring the phosphorylation level of poly-Glu-Ala-Tyr-biotin (pGAT-biotin) peptide in a Homogenous Time-Resolved Fluorescence (HTRF) assay. Into a black 96-well Costar plate is added 2 μl/well of 25× compound in 100% DMSO (final concentration in the 50 μl kinase reaction is typically 1 nM to 10 μM). Next, 38 μl of reaction buffer (25 mM Hepes pH 7.5, 5 mM $MgCl_2$, 5 mM $MnCl_2$, 2 mM DTT, 1 mg/ml BSA) containing 0.5 mmol pGAT-biotin and 3–4 ng KDR enzyme is added to each well. After 5–10 min preincubation, the kinase reaction is initiated by the addition of 10 μl of 10 μM ATP in reaction buffer, after which the plate is incubated at room temperature for 45 min. The reaction is stopped by addition of 50 μl of KF buffer, (50 mM Hepes, pH 7.5, 0.5 M KF, 1 mg/ml BSA) containing 100 mM EDTA and 0.36 μg/ml PY20K (Eu-cryptate labeled anti-phosphotyrosine antibody, CIS bio international) is added and after an additional 2 h incubation at room temperature, the plate is read in a RUBYstar HTRF Reader.
23. Cell-based assay for VEGFR-2 inhibition: (i) *Transfection of 293 cells with DNA expressing FGFR1/VEGFR-2 chimera*: A chimeric construct containing the extracellular portion of FGFR1 and the intracellular portion of VEGFR-2 was transiently transfected into 293 adenovirus-transfected kidney cells. DNA for transfection was diluted to a 5 μg/ml final concentration in a serum-free medium and incubated at room temperature for 30 min with 40 μl/mL of Lipofectamine 2000, also in serum-free media. 250 μl of the Lipofectamine/DNA mixture was added to 293 cells suspended at 5×10^5 cells/ml. 200 μl/well of the suspension was added to a 96-well plate and incubated overnight. Within 24 h, media was removed and 100 μl of media with 10% fetal bovine serum was added to the now adherent cells followed by an additional 24 h incubation. Test compounds were added to the individual wells (final DMSO concentration was 0.1%). Cells were lysed by re-suspension in 100 μl Lysis buffer (150 mM NaCl, 50 mM Hepes pH 7.5, 0.5% Triton X-100, 10 mM NaPPi, 50 mM NaF, 1 mM Na_3VO_4) and rocked for 1 h at 4 °C.(ii) *ELISA for detection of tyrosine-phosphorylated chimeric receptor*: 96-well ELISA plates were coated using 100 μl/well of 10 μg/ml of αFGFR1 antibody, and incubated overnight at 4 °C. αFGFR1 was prepared in a buffer made with 16 ml of a 0.2 M Na_2CO_3 and 34 ml of a 0.2 M $NaHCO_3$ with pH adjusted to 9.6. Concurrent with lysis of the transfected cells, αFGFR1 coated ELISA plates were washed three times with PBS + 0.1% Tween-20, blocked by addition of 200 μl/well of a 3% BSA in PBS for 1 h and washed again. 80 μl of lysate were then transferred to the coated and blocked wells and incubated for 1 h at 4 °C. The plates were washed three times with PBS + 0.1% Tween-20. To detect bound phosphorylated chimeric receptor, 100 μl/well of anti-phosphotyrosine antibodies (RC20:HRP), Transduction Laboratories)) were added (final concentration 0.5 μg/ml in PBS) and incubated for 1 h. The plates were washed six times with PBS + 0.1% Tween-20. Enzymatic activity of HRP was detected by adding 50 μl/well of equal amounts of the Kirkegaard & Perry Laboratories (KPL) Substrate A and Substrate B. The reaction was stopped by addition of 50 μl/well of a 0.1 N H_2SO_4, absorbance was measured at 450 nm.